

## ANALYSIS AND MODELLING OF GLASS MELTING

LUBOMÍR NĚMEC

Laboratory of Glass and Ceramic Materials, Institute of Chemical Technology and  
Academy of Sciences of Czech Republic, Technická 5, 166 28 Praha 6

## INTRODUCTION

In overlooking the glass melting process, three research activities in the field may be noticed:

1. Improvement and new ways of glass melting
2. Automatic process control by models
3. Identification and elimination of glass melting defects.

The aim of this paper is to present and evaluate some interesting trends in the above mentioned areas. The scope of the paper will be restricted to the processes taking place within the glass melt and to their deterministic theoretical models.

## 1. IMPROVEMENT AND NEW WAYS OF GLASS MELTING

It is well known that the glass melting process is controlled mainly by mass transfer. While the effect of temperature has been almost profitted, glass convection is employed mainly in its natural form. In the following paragraphs, an attempt is made to explain the influence of controlled glass convection on the course of melting processes with the intention to open a way for its future application.

## 1.1. Energy consumption of the glass melting process

Energy consumption gives instructive information about the process efficiency. A detailed discussion of this subject is given e.g. by Cooper [1].

Considering convection influence on the particle dissolution resp. glass homogenization, the value of  $\text{grad } v$  is significant, where  $v$  is glass velocity. Assuming a reciprocal dependence between throughput  $\dot{M}$  and time to accomplish the process  $\tau$ , the following equation may be proposed:

$$\tau = \frac{\tau^0}{1 + K^c \text{grad } v} \quad (1)$$

where  $\tau^0$  is valid for  $\text{grad } v = 0$  and  $\tau \rightarrow 0$  as  $\text{grad } v \rightarrow \infty$  and  $K^c$  is constant at the given temperature. The formula for the specific energy consumption  $H_M^0$ , not considering any heat recycling and involving the time factor [2,3], has the form:

$$H_M^0 = \frac{(\alpha T^m - T^{\text{ex}}) A K^{\text{Cr}} \tau^{\text{Cr}}}{\sum \delta_i / \lambda_i V^a \rho} + \int_{T^e}^{T^m} C^g dT + H_M^g \quad (2)$$

where  $\alpha$  expresses the simplified relation between maximum melting temperature and temperature of inner surfaces,  $T^m$  and  $T^{\text{ex}}$  are the maximum and outer surface temperatures respectively,  $A$  is the overall boundary surface,  $\delta_i$  and  $\lambda_i$  are thickness and thermal conductivity of the  $i$ -th refractory layer, respectively, and  $\rho$  is the average glass density. The necessary residence time of glass is represented by the expression  $K^{\text{Cr}} \tau^{\text{Cr}}$ , where  $\tau^{\text{Cr}}$  is the residence time on the critical path,  $V^a$  is the active volume of the melting room and  $K^{\text{Cr}} = \bar{\tau} / \tau^{\text{Cr}}$  where  $\bar{\tau}$  is the average residence time,  $C^g$  is the specific heat per unit mass of glass, and  $H_M^g$  is the reaction heat of the reactions in the glass batch, the vaporization heats and the enthalpy to heat the glass and gases to  $T^e$ .

Using eq. (1) analogical to Cooper's relation [1] and eq. (2), the effect of temperature and glass convection may be represented by equations (3) and (4), respectively:

$$\frac{\partial H_M^0}{\partial T^m} = -K_1 (\alpha T^m - T^{\text{ex}}) \frac{K^T}{T^{m2}} \exp \frac{K^T}{T^m} + K_1 \alpha \exp \frac{K^T}{T^m} + C^g \quad (3)$$

$$\frac{\partial H_M^0}{\partial \text{grad } v} = K_2 \left[ -\frac{K^{\text{Cr}} K^c}{V^a (1 + K^c \text{grad } v)^2} - \frac{K^{\text{Cr}}}{V^a (1 + K^c \text{grad } v)} \frac{\partial V^a}{\partial \text{grad } v} + \frac{1}{V^a (1 + K^c \text{grad } v)} \frac{\partial K^{\text{Cr}}}{\partial \text{grad } v} \right] \quad (4)$$

where  $K_1$  and  $K_2$  are both positive.

The first term on the right-hand side of equation (3) involves the influence of the increased output and is negative. However, when  $T^m \rightarrow \infty$  the value of the term approaches zero. The second and third terms are always positive, i.e. at very high temperatures,  $H_M^0$  may slightly grow with temperature. Applying controlled convection, not only the melting time but also the flow distribution i.e. the values of  $V^a$  and  $K^{\text{Cr}}$  are expected to be strongly influenced. The first term on the right-hand side of eq. (4) expressing the influence of the increased output is always negative.

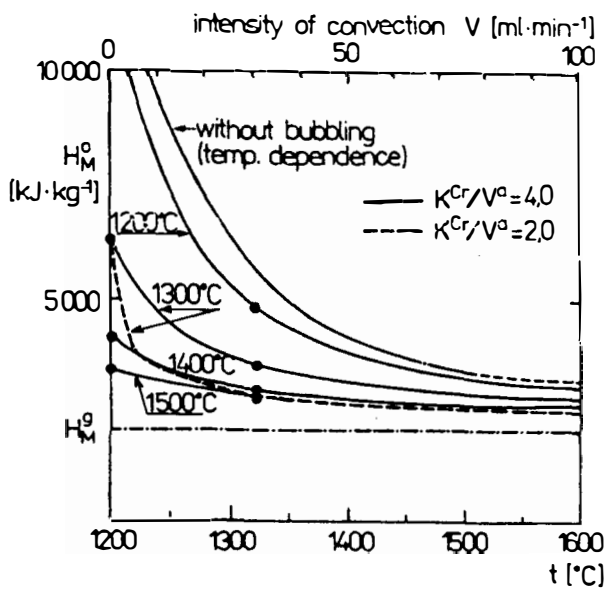


Fig. 1.: The dependence between specific energy consumption of glass melting  $H_M^0$  and temperature resp. intensity of glass convection.  $V$  - the volume rate of oxygen bubbled through the laboratory melt (is supposed to be proportional to  $\text{grad } v$ ).

For  $\text{grad } v \rightarrow \infty$ , the value of this term goes to zero. The second and third terms are negative only if  $V^a$  is growing and  $K^{Cr}$  is decreasing with convection intensity, i.e. with proper arrangement of glass convection. As  $K_2$  is decreasing with growing maximum temperature and also  $K^c$  shows a slight decrease, the value of the whole first term in eq. (4) is slightly growing with decreasing temperature, i.e. medium or lower temperatures are advantageous for controlled convection application. Refining, however, is probably not accelerated.

Fig. 1 shows the calculated dependences between specific energy consumption of soda-lime glass and temperature as well as convection intensity in a melting tank. Laboratory experimental values of  $\epsilon$  and dissolving times have been applied for the calculation of  $H_M^0$ . In experiments with controlled convection, oxygen has been bubbled into the melting pot. Due to the impossibility to measure the values of  $\text{grad } v$ , proportionality between the rate of gas bubbling  $\dot{V}$  and  $\text{grad } v$  is supposed.

As obvious from Fig. 1, the decrease in  $H_M^0$  with  $\dot{V}$  ( $\text{grad } v$ ) is steeper at lower temperatures as already predicted. The comparison with temperature dependence of  $H_M^0$  (the curve without bubbling) reveals that the application of controlled convection provides theoretically lower values of  $H_M^0$  due to the lower lower of maximum temperature.

## 1.2. Batch reactions and particle dissolution

Hrma in his detailed reviews [4,5] distinguishes three reaction stages: reactions in the solid phase, reactions in the liquid phase and dissolution of refractory particles in the melt.

In the first stage, the application of careful batch mixing is more important before melting; during melting, the gas evolution may be accelerated by convection but tight contact of reactants seems to be of greater importance.

During the second stage, dissolution of solid materials in the melt, chemical reaction, gas evolution and precipitation as well as dissolution of crystalline compounds take place. In the later time period controlled by diffusion of  $\text{SiO}_2$  in the melt, the amount of the melt changes with the amount of precipitated crystals according to melting conditions and, consequently, the thickness of the diffusion layer on grain surfaces changes. Temperature has only a slight influence as the portion of melt and, consequently, the diffusion layer thickness  $\delta$  grows with temperature [4]. Melt convection has a favourable effect especially after decarbonization, where dissolution of sand grains is accelerated and permits creation of only thin diffusion layers around sand grains. When polydisperse commercial sands are used, the sands with broad size distribution and high portions of fine grains dissolve with the most difficulties.

During the third stage, only glass melt, bubbles and refractory particles are present. A new generation of refractory particles is produced on the furnace boundaries attacked by corrosion. The process of all particles dissolution is controlled by mass transfer and the equation describing the rate of particle dissolution is:

$$\dot{r} = -\alpha(w_e - w_m) \quad (5)$$

where  $w_e$  is the equilibrium mass fraction of  $\text{SiO}_2$  in the glass melt and  $w_m$  is the mass fraction of  $\text{SiO}_2$  in the melt. While the value of  $w_m$  may be easily expressed from the mass balance of  $\text{SiO}_2$  [6], the coefficient of mass transfer  $\alpha$  is a complicated function of batch granulometry, glass composition, melting geometry and temperature as well as flow history over the whole melting period:

$$\alpha = \alpha[f(r), g(w_i), h(x, y, z), v(\tau), T(\tau)] \quad (6)$$

It is, however, not feasible to obtain a general solution of equation (6).

The refractory particles of the second generation, such as  $\text{Al}_2\text{O}_3$ ,  $\text{ZrO}_2$  or  $\text{Cr}_2\text{O}_3$  having its origin in the refractory material corrosion, have a much simpler history. Here,  $f(r) = r_0$ ,  $g(w_i) \rightarrow 0$ ,  $h(x, y, z)$  is neglected (single particle),  $T(\tau)$  may be obtained from flow modelling and  $v(\tau)$  involves the influence

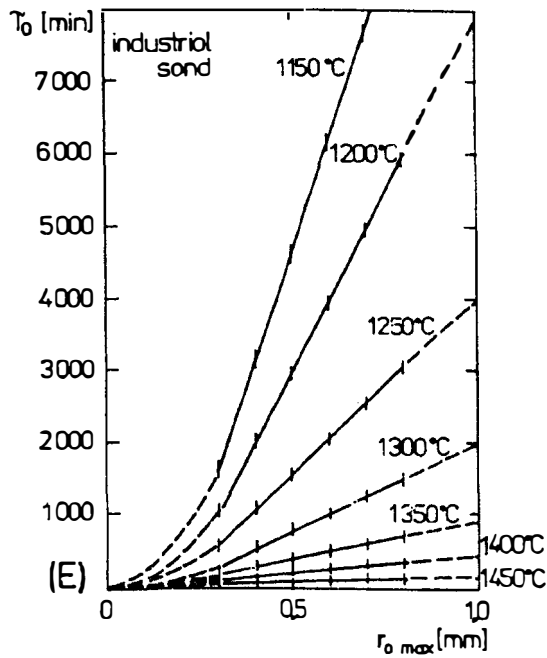


Fig. 2.: Dependence of dissolution time of sand on  $r_{0max}$  at temperatures indicated (37% cullet) for industrial sand.

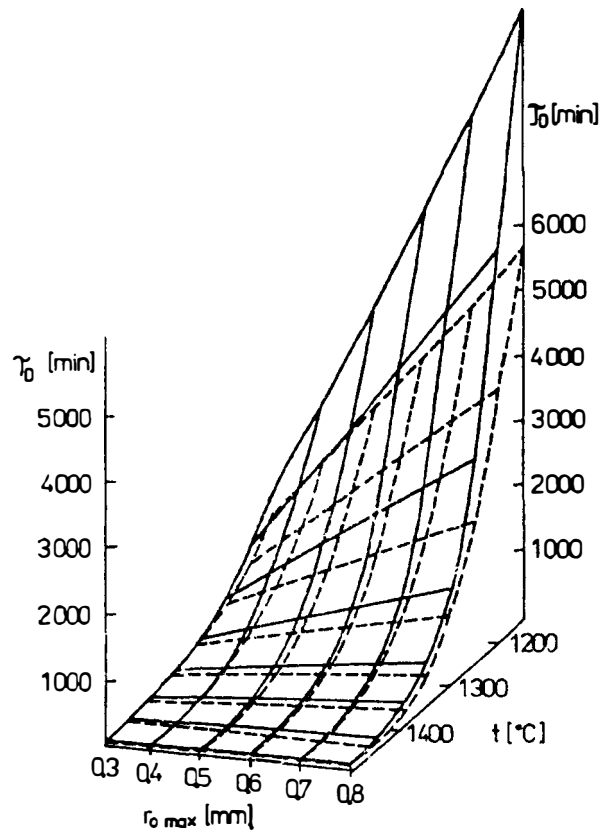


Fig. 3.: Influence of  $r_{0max}$  and temperature on time of sand dissolution in three-dimensional representation:  $r_{0max} = 0.5$  mm, 37% cullet. Upper surface represent industrial sand, lower surface monodispersion.

of free convection. The laboratory experiments are able to simulate acceptably the furnace melting conditions. The solubilities of  $Al_2O_3$ ,  $ZrO_2$ ,  $SnO_2$  and  $Cr_2O_3$  in soda-lime glass as a function of temperature are given in the work of Manfredo and McNally [7], the values of effective binary diffusion coefficients of  $Al_2O_3$  are given in [8,9], those of  $SiO_2$  in  $K_2O-SiO_2$  and  $Na_2O-SiO_2$  melts or in  $Na_2O-SiO_2$  melt are presented in [10-12].

The refractory particles of glass batch undergo, however, a much more complicated history. Nevertheless, the important features of the reaction mechanism involving the reaction path, the rate of production of  $CO_2$ , the rate of silica dissolution during and after  $CO_2$  evolution and the influence of initial silica concentration and temperature on the process rate and control are described in details in Hrma's work [13,14].

The analysis of Beneš's results [15] given by Hrma, Bartoň and Tolt [16], showed the influence of the initial heating and reaction period on the rate of monodisperse sand dissolution even at isothermal conditions between 1250-1410°C in container glass. The unexpected temperature dependence between 1250-1410°C as well as dissolution problems with commercial sands with broad size distribution have been explained by the amount of silica consumed during the first period of dissolution. The sudden dissolution increase at 1410°C has been attributed to convection effect of the refining bubbles. The direct cor-

relations between the sand dissolution times and the rate of bubble growth (being in relation with bubble nucleation and bubble convection) in soda-lime glass refined by  $Na_2SO_4$ ,  $As_2O_3 + NaNO_3$  and  $NaCl$ , respectively, have been found in [17].

Considering polydisperse silica grains, the value of undissolved sand portion  $w_s(\tau)$  may be expressed using the probability density function  $f(r)$  [18]:

$$w_s = \frac{4}{3} \pi \rho_s n_{S0} \int_0^{r_{max}} f(r + r_{0max} - r_{max}) r^3 dr \quad (7)$$

where  $\rho_s$  is silica density,  $n_{S0}$  is the initial number of sand particles in mass unit and  $r_{max}$  is the size of maximum sand particle in time  $\tau$ . For the  $\alpha$  relation, the simplified expression has been used involving three semiempirical coefficients  $\alpha_0$ ,  $\alpha_f$  and  $\kappa$  being dependent only on the temperature [6]. Thus, only states having a similar time-temperature history, resulting glass composition and batch granulometry may be compared. In Fig. 2, the dependence is given of  $\tau_D$  on  $r_{0max}$  and the temperature, respectively, presenting temperature influence and linear dependence between  $\tau_D$  and  $r_{0max}$  in a broad range of  $r_{0max}$  val-

Table I

Controlling processes and main factors influencing silica dissolution during batch melting

Stage	Controlling processes	Main influencing factors
stage before melt appearing	gas evolution, nucleation, surface and volume diffusion heat transfer	rate of heating, contact of reactants, silica (batch) amount and granulometry, batch homogeneity
reactions in melt	gas evolution (earlier stage), mass transfer, heat transfer (rapid heating), viscous flow	$p_{CO_2}$ , temperature history, silica amount and granulometry, melt convection, temperature (slight influence)
dissolution of refractory particles	mass transfer	temperature history, temper. (slight infl. up to ref. temperatures), silica amount and granulometry, refining agents, melt convection (distinct influence)

ues as well as for polydisperse sand. The influence of  $\tau_D$  values on the  $f(r)$  presented in Fig.3 and further results show that at a given value of  $r_{0max}$ , monodispersion is the most advantageous [18].

As may be expected, convection accelerates essentially sand dissolution in the later stages. The influence of oxygen bubbling into the laboratory soda-lime glass melt has been investigated in [19] using  $Na_2SO_4$ ,  $As_2O_3 + NaNO_3$  or  $NaCl$  as the refining agents. As an example, the pronounced decrease in  $\tau_D$  at lower temperatures can be shown (Fig.4), when bubbling  $O_2$  through the melt has been applied on laboratory scale.

Inspection of Table I reveals the promising role of convection in the second and especially in the third stages of melting. For the given state of glass furnace, the maximum pull  $\dot{M}$  may be based on the heat transfer -  $\dot{M}_H$ , or mass transfer -  $\dot{M}_M$  [20]. Thus, if  $\dot{M}_H \gg \dot{M}_M$ , melting is controlled by mass transfer and vice versa. The total heat flow into the glass batch is given by:

$$\dot{H}^0 = \dot{M}_H [H_M^g + C^g(T^m - T^e)] \quad (8)$$

where terms in brackets are given by eq. (?).  $H^0$  may be expressed as the heat flow into the glass batch from both sides:

$$\dot{H}^0 = \lambda_{ef}^g A^l (T^{mg} - T^l) / \delta_g + \lambda_{ef}^c A^u (T^{mc} - T^u) / \delta_c \quad (9)$$

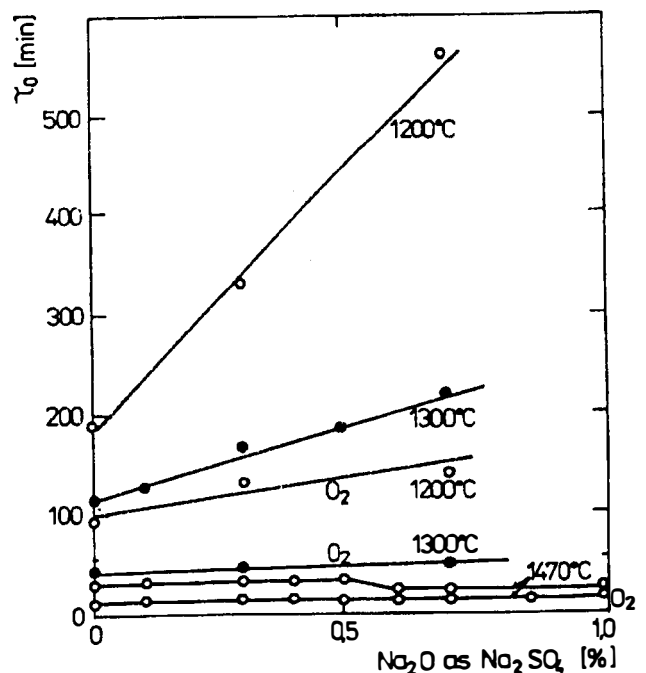


Fig. 4.: The influence of oxygen bubbling ( $30 \text{ ml min}^{-1}$ ) and refining agent concentration on the sand dissolution time in soda-lime glass.  $r_{0max} = 0.5 \text{ mm.}$ ,  $O_2$  designates application of bubbling.

And combining both equations we obtain:

$$\dot{M}_H = \frac{\lambda_{ef}^g A^l (T^{mg} - T^l) / \delta_g + \lambda_{ef}^c A^u (T^{mc} - T^u) / \delta_c}{H_M^g + C^g (T^m - T^e)} \quad (10)$$

where  $\lambda_{ef}$  is the effective heat conductivity and the indices have the following significances: g – glass, c – combustion gases, l – lower surface of glass batch, u – upper surface of glass batch, m – maximum, e – exit. The value of  $\dot{M}_M$  may be defined using the expression for the so-called fining layer. The “thickness” of the fining layer may be expressed as a fraction of the characteristic size of furnace  $\delta_f = \beta L$  (where  $\beta \leq 1$  and  $L$  may be the length or the height of the furnace). The pull  $\dot{M}_M$  may be written as  $\rho \bar{v}_L S^a$ , where  $\bar{v}_L$  is the average velocity of glass movement in the direction of the characteristic size and  $S^a$  is the active cross section through the furnace. Because  $\bar{v}_L = \frac{\beta L}{\tau} = \frac{\beta L}{K^{Cr} \tau^{Cr}}$  (see eq. (2)), the value of  $\dot{M}_M$  is given by:

$$\dot{M}_M = \frac{\rho V^a}{K^{Cr} \tau^{Cr}} \quad (11)$$

where  $\beta L S^a = V^a$ .

The temperature growth enhances the value of  $\lambda_{ef}$  as well as  $T^m$  and lowers the value of  $\tau^{Cr}$ , therefore both  $\dot{M}_H$  and  $\dot{M}_M$  are growing. The further temperature rise is limited by the materials of the walls and electrodes as well as by glass evaporation. Furthermore, increasing temperatures of both batch surfaces and a growth of the second term in the denominator limit a further increase in  $\dot{M}_H$ . At the same time, the value of  $\dot{M}_M$  grows because of the  $\tau^{Cr}$  decrease (see Fig. 4) and probably also because of the  $V^a$  value increase and  $K^{Cr}$  decrease.

Application of glass convection at medium temperatures leads to the growth of  $\lambda_{ef}^g$  values, and decrease in  $\delta_g$  but  $T^l$  may also grow. If a more intensive convection is allowed, a portion of the batch in the reacting layer is torn off and mixed with the melt. An additional term expressing the very intensive heat transfer from the glass into the submerged batch particles may be inserted into the numerator of eq. (10):  $\lambda_{ef}^g A^b (T^m - T^b) / \delta_g$ , where  $A^b$  is the entire surface of the submerged glass batch. At an extremely high intensity of glass convection, no glass batch remains on the glass level; the first term in the numerator of eq. (10) will be substituted for the heat flow from the glass melt to the total amount of submerged glass batch. Heat transfer from the combustion room will also increase as the  $T^u$  value decreases.

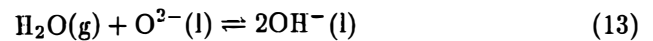
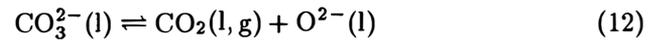
Despite these promising theoretical results, the application of controlled convection is hampered by some practical problems. 1. How to reach an intensive convection and how to arrange it. 2. How to ensure a good ispersion of batch in glass and at the same

time provide a sufficient residence time in the glass furnace (see [21] f.e.). (The batch feeding under the glass level opens here another theoretical possibility of batch dispersion). 3. How to conserve the beneficial effect of high alkali melt in the earlier melting stages.

### 1.3. Refining

Although reliable estimates of the initial bubble compositions may be obtained from experimental measurements [22–24], no general theory of bubble generation at earlier stages exists and only scanty data are found in the literature about nucleation and growing mechanisms [25,26]. The refining process in the stage of single bubbles, however, has been more accessible to experiments [17,27]; this fact led to a simplified mathematical description of the process [28,29] and determination of the significant refining factors in this stage [30].

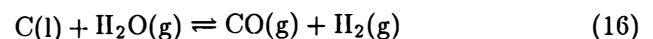
It is well known that chemical equilibria and solubilities of gases in glass, reactions producing gases and the corresponding mutual reaction of gases play an important role in the later refining stages. The following brief reaction review attempts to illuminate this problem. Several categories of bubbles arise from the glass melting process: bubbles from batch decomposition, bubbles nucleated in later stages, bubbles from pores of solid materials, bubbles generated by chemical and electrochemical reactions and bubbles generated mechanically. Two important equilibria dominate the batch reactions:



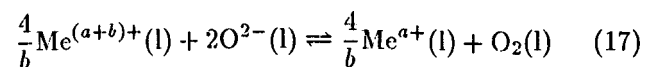
However, reactions of refining agents are also taking place, especially on sand particles (see later), and added salts decompose:



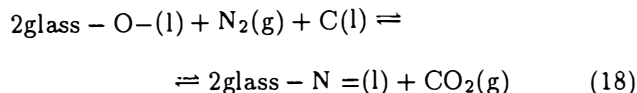
In the presence of organic and reducing components dissolved in the glass:



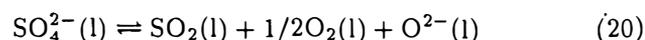
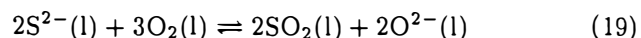
Simplifying the complicated oxidation reactions at lower temperatures [31,32], the general equation of refining oxidation-reduction pairs may be written as:



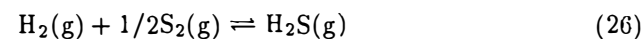
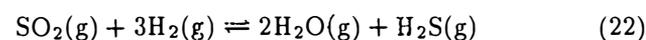
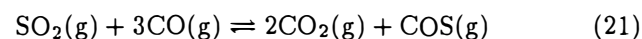
Nitrogen is physically dissolved, at reduction conditions however, the following reaction takes place [33]:



As Richardson claims [34], the following two reactions of sulphur compounds define the reduction and oxidation state of the glass melt:



To define the oxidation-reduction states of the atmosphere (bubbles) in more details, possible reactions with current impurities must be taken into account. Jebesen-Marwedel and Brückner [35] present a whole range of reactions producing  $\text{SO}_2$ ,  $\text{CO}_2$ ,  $\text{H}_2$ ,  $\text{CO}$  and  $\text{H}_2\text{O}$ , respectively. Some gas products may subsequently react as follows:



As a result,  $\text{H}_2\text{S}$  and  $\text{COS}$  may be found in bubbles [36], sulphur is present only in absence of both  $\text{H}_2$  and  $\text{CO}$ . Including reactions (21-26), the following oxidation-reduction states of the gas phase may be proposed:

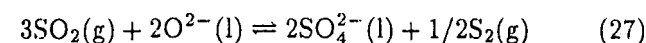
Strongly reduction state where  $\text{CO}$  and  $\text{H}_2$  or  $\text{H}_2\text{S}$  and  $\text{COS}$  (in presence of sulphur compounds) are present in the atmosphere or bubbles.

Slightly reduction state, where only  $\text{H}_2\text{S}$  and  $\text{COS}$  are present in the gas phase as well as sulphur (defined only for melts with sulphur compounds).

Neutral state, where  $\text{SO}_2$  and sulphur are present in the gas phase (defined only for melts with sulphur compounds).

Oxidation state, which is characterized by oxygen presence in the gas phase.

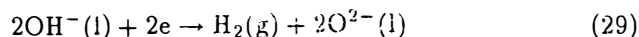
if an oxidation state exists in the melt phase and a neutral state in the gas phase, the disproportionation reaction according to Golob and Swarts [37] takes place:



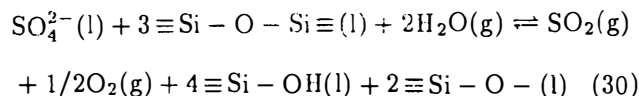
The list of the reactions would not be complete if electrochemical reactions were not considered [38]:



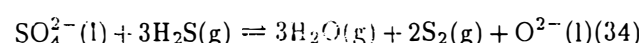
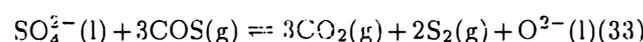
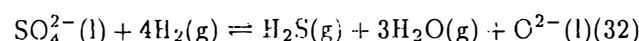
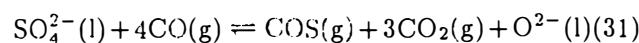
At low current frequencies, Matěj [39] has observed hydrogen evolution on the Mo electrode:



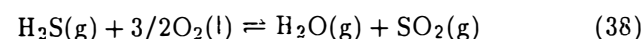
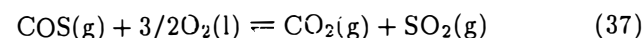
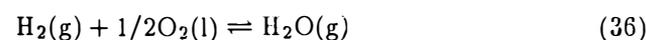
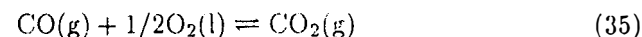
The influence of wet atmosphere involves a competition reaction between  $\text{SO}_4^{2-}$  and  $\text{OH}^-$  ions [40]:



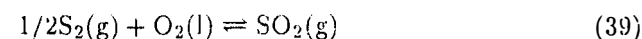
Consequently, this reaction is influenced by the presence of oxidation-reduction pairs [41]. In reality, an arbitrary combination of oxidation-reduction states of the atmosphere (bubbles) and glass may result in the following proposed reactions. In glasses containing the sulphur compounds:



In the gas phase reactions (25-26) occur. Reactions of dissolved  $\text{SO}_2$  (21-24) and, consequently, (25-26) also take place. Reactions with oxygen for all types of glasses correspond to:



In absence of both  $\text{CO}$  and  $\text{H}_2$ , sulphur reacts with oxygen:



Contrary to sulphates and oxides, no chemical reactions with gases in bubbles are expected when halogenides are used as refining agents. Reactions (35-36) are only taking place in the strongly reducing bubbles.

When formulating the sets of equations controlling the bubble behaviour in glass, the low sulphate solubility leading to its precipitation on the boundaries (bubbles) should be also taken into account [42,43] if necessary.

The behaviour of the multicomponent gas bubble in a liquid may be described as [30]:

$$\sum_{i=1}^n p_i \geq \sum_{i=1}^n p_{i\text{melt}} \quad (40)$$

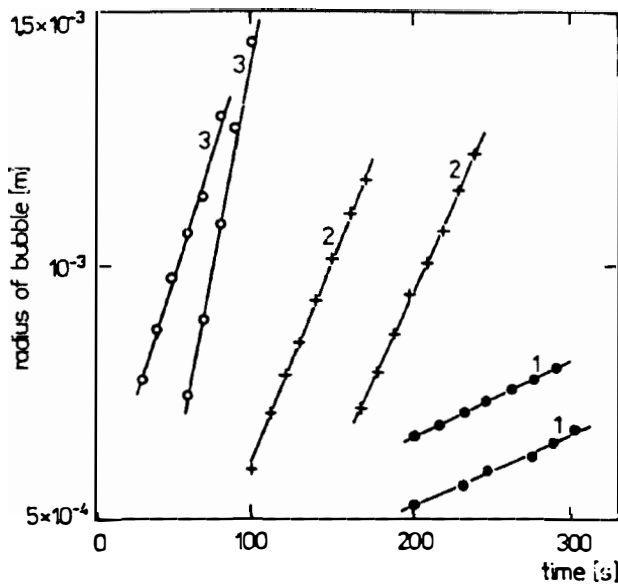


Fig. 5.: The experimental relationship between bubble radius and time in a soda-lime glass melt obtained by high temperature photography.  
 Curve 1: refining agent 1% As<sub>2</sub>O<sub>3</sub> + 1% Na<sub>2</sub>O as NaNO<sub>3</sub> at 1450° C  
 Curve 2: refining agent 1% Na<sub>2</sub>O as Na<sub>2</sub>SO<sub>4</sub> at 1470° C  
 Curve 3: refining agent 1.5% NaCl at 1530° C

where  $p_i$  is the partial pressure of the  $i$ -th gas in the bubble while  $p_{imelt}$  is its equilibrium partial pressure in the melt. If the sign  $>$  is valid in eq. (40), the bubble dissolves, but dissolution stops in the presence of at least one almost nondiffusing gas (nitrogen). Thus, bubble dissolution may only be exceptionally accepted as the refining mechanism. If, on the contrary, the lower sign holds, the bubble grows and subsequently is quickly removed from the glass [27]. (see Fig.5) The difference between  $\sum p_{imelt}$  and  $\sum p_i$  can be used therefore as the criterion of refining ability.

The possible ways of accelerating the refining process result also from eq. (40) (sign  $<$  is valid).  
 Temperature influence: Growing temperature enhances the value of  $\sum p_{imelt}$  due to the decreasing stability of the complex ions in question.  
 Refining agent presence and its concentration: Refining agents exhibit distinctly high values of  $p_{imelt}$  of their gas products. At a given temperature, the product pressures are growing within certain limits with refining agent concentration in glass [17], (eqs.(17), (20)).  
 Choice of refining agent: The chemical bond of the refining ion in glass significantly influences the value of the respective  $p_{imelt}$  [44].  
 Influence of glass composition: The growing glass ba-

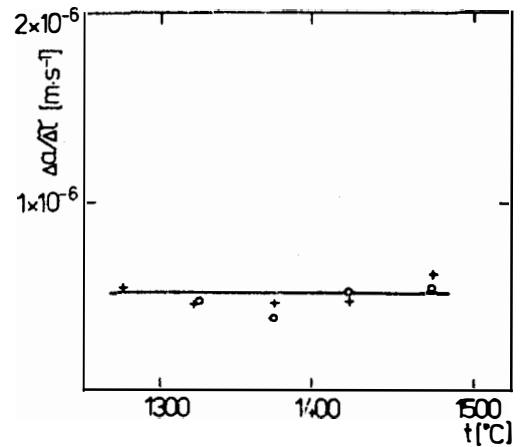


Fig. 6.: The dependence between the value of bubble growth rate,  $\Delta a/\Delta \tau$ , and temperature.

$t$ [°C]	+ with refining agent	o without refining agent
1275	5 kPa	< 1 kPa
1325	20 kPa	3 kPa
1375	40 kPa	15 kPa
1425	85 kPa	20 kPa
145	135 kPa	30 kPa

Table II

The experimental values of average bubble growth rates corresponding to the effective refining ( $\tau_{Ref}$  is about 10 min) of soda lime glass (74 wt.% SiO<sub>2</sub>, 16 wt.% Na<sub>2</sub>O, 10 wt.% CaO) refined by different refining agents [34]

	Refining agent	Temper. [°C]	$\Delta a/\Delta \tau$ exp. [ms <sup>-1</sup> ]
1	1% As <sub>2</sub> O <sub>3</sub> + 1% NaNO <sub>3</sub>	1400	$7.3 \times 10^{-7}$
2	1% As <sub>2</sub> O <sub>3</sub> + 1% NaNO <sub>3</sub>	1450	$8.5 \times 10^{-7}$
3	0.4% Na <sub>2</sub> O as Na <sub>2</sub> SO <sub>4</sub>	1470	$1.2 \times 10^{-6}$
4	0.5% Na <sub>2</sub> O as NaCl	1530	$7.0 \times 10^{-7}$

sity enhances the refining ion solubility in glass and thus supports its efficiency.

Pressure influence: Decreasing pressure lowers the value of  $\sum p_i$ , thus accelerating the bubble growth, pressure increase supports bubble dissolution (eq.(40)) (though incomplete).

Among bubble size, glass viscosity and thickness of the refined glass layer as the main factors influencing the refining, the instantaneous bubble size has the decisive significance. As shown in Fig.6 [45] and in Table II [17], similar values of bubble growth rate  $\Delta a/\Delta \tau$  (about  $10^{-6} \text{ms}^{-1}$ ) have been found for refin-

ing at different temperatures, pressures, for different temp. regimes, refining agents and glasses. As obvious from these results, every component present in the glass able to produce a quickly diffusing gas or vapour of partial pressure comparable with the total pressure in the melt, ensures successful refining. E.g. carbon dioxide shows to be a sufficiently effective refining gas at reduced pressures and relatively low temperatures between 1250–1350°C.

As bubbles move in glass owing to gravitational, centrifugal or surface forces, the significance of glass convection for gas diffusion into bubbles seems to be restricted. Under conditions of the turbulent glass stirring, bubbles may be finally concentrated in the glass layer just under the glass level and only a small amount of them will be removed by bursting on the glass level.

Therefore, an additional refining must be used especially at medium temperatures and in absence of refining agents. If a less vigorous glass stirring is applied such as slow rotation, the refining time is not expected to be significantly influenced.

#### 1.4. Homogenization

The composition (intensity), shape size and orientation of heterogeneities from the glass batch are the complex functions of input quantities and history as given in eq.(6). A new generation of heterogeneities with a simple history occurs in the glass melting furnace owing to evaporation, corrosion and phase segregation. Two approaches are applied to evaluate a homogenizing action of a melting room.

The first conception considers the overall mixing ability of a melting room employing the transient characteristics of the melting furnace [46–48] or the residence time distributions which may be obtained from computer models by streak line techniques [49–51] or by simulating tracer experiments [52,53]. Using these characteristics, the shortest residence time, the average residence time, the active melting volume and the amplitude of concentration fluctuations may be obtained.

Combining basic models of flow – the ideal mixer and the ideal plug flow – the transient characteristics may be modelled as combinations of these models. Taking into account the fundamental flow requirements, the ideal mixing and ideal plug flow may be evaluated as follows:

1. Fast going melting process: For the ideal mixer,  $\tau_D$  (dissolution time of particles)  $\rightarrow \tau_{CH}$  (time of chemical reactions, nucleation, gas evolution and heat transfer, respectively),  $\tau_H$  (homogenization time)  $\rightarrow 0$  as  $\delta_H$  (the thickness of the heterogeneity)  $\rightarrow 0$ ,  $\tau_R$  (refining time) is usually not shortened (see Refining). For the ideal plug flow,  $\tau_D$  and  $\tau_H$  have high values,  $\tau_R$  is unaffected.

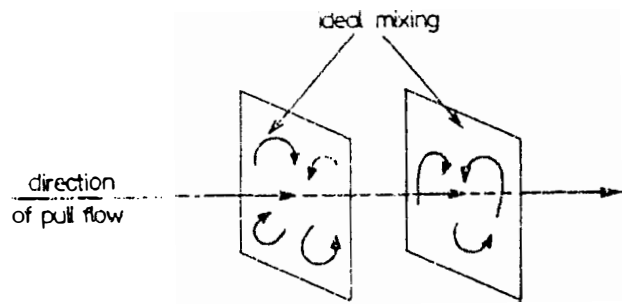


Fig. 7.: Representation of the formation of "quasi-plug flow".

2. High degree of melting volume utilization. For both flow models,  $V^a \rightarrow V$  (full utilization).

3. The equal or compensated time - temperature history of glass elements. For the ideal mixer, the broadest, most disadvantageous, residence time distribution ( $\tau^{Cr} \rightarrow 0$ ) exists. For the ideal plug flow, all histories are equal.

To combine benefits of both models, the glass flow could be proposed where the plug flow is simulated in the direction of throughput and ideal mixing in the perpendicular direction as is obvious from Fig.7. As already mentioned, refining requires separate treatment with possible application of physical methods (refining at reduced pressures). Realization of this "quasi-plug flow" meets however serious obstacles and may be only partially successful using special mixing elements, heating and bubbling. In Fig. 8b, helical streak lines of glass elements are shown in a horizontal melting room with only a longitudinal temperature barrier close to the right-hand wall. In comparison with the classical transversal barrier, the minimum residence time grew up from 229 min to 490 min ( $\tau = 1326$  min) and the very similar average temperatures of streak lines were obtained. Another possibility of an intensive mixing of glass and restriction of the vast longitudinal flows consists in a series of mixers with several transversal rows of bubbling nozzles [54] or heating elements (see Fig.8c), or in similar flow simulation in a vertical furnace (see Fig.8a). The simulation of "ideal" flows can be considered one of the promising opportunities for simple computer models of melting rooms. Cooper [55] underlines in his work the urgent need of criteria enabling to find such optimum flow behaviour.

The second approach to the homogenization process treats heterogeneities as objects having composition, viscosity and surface tension different from the surrounding glass. The disappearance of heterogeneities proceeds as a consequence of diffusive mixing and heterogeneity deformation by glass flow.

The overall heterogeneity may be considered as

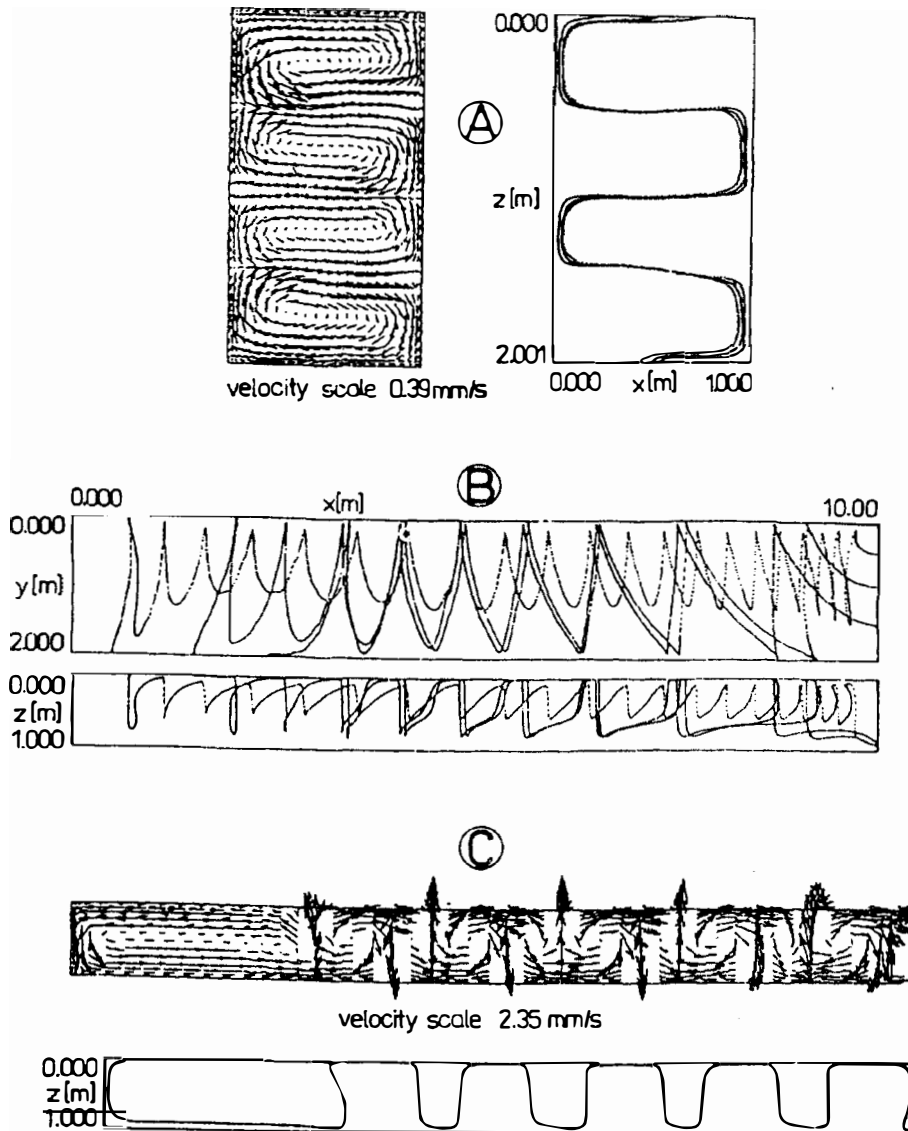


Fig. 8.: The examples of velocity fields and streak lines in a rectangular glass melting room.

- a) vertical throughput flow ( $y = 0.5$  m),
- b) longitudinal temperature barrier ( $y = 1.9$  m),
- c) five transversal temperature barriers ( $y = 1.9$  m).

a series of fluctuations of concentration  $C$  about its mean value  $\bar{C}$ . From the solution of the diffusion equation it is obvious [56] that diffusion always lowers the heterogeneity amplitude  $C - \bar{C}$ , the rate of the  $C - \bar{C}$  decrease depends on the value of  $\delta_i^2$  and diminishes with time. All kinds of heterogeneities - spherical, striated and laminated [57] are subject to deformations, but higher viscosity and surface tension of heterogeneities slow down the homogenization process. Deformations are caused by shear and streamline attenuation (rotation). As Cooper shows [57] shear is most effective if heterogeneity is initially perpendic-

ular to streamlines, but rotation with rotation axis perpendicular to glass flow (the reduction of the cross area), on the contrary, reduces strongly the characteristic size when the heterogeneity is initially parallel to streamlines. The fact that opposite orientation of heterogeneity is required both for shear and rotation as well as the fact that deformation decreases with time lead to preference of systems producing a variety of flows with differently scaled, positioned and oriented circulations [57].

Both approaches obviously lead to similar requirements consisting mostly in the evocation of circula-

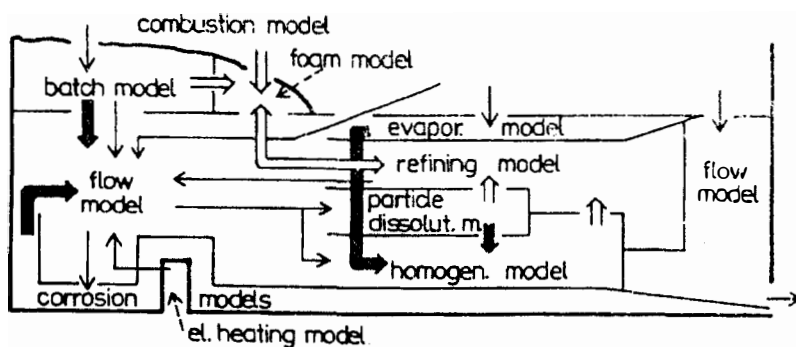


Fig. 9.: The complex mathematical model for the glass melting process control.

- ➔ production of refr. particles, bubbles and heterogeneities,
- ➔ production of heterogeneities,
- ➔ production of foam or bubbles,
- ➔ the main direct influences.

tion flows and in initiating an intensive like turbulent flow especially in the vertical and transversal directions. As mentioned above, the application of controlled convection accelerates also distinctly sand dissolution, may promote batch reactions and improves the volume utilization of the glass furnace.

## 2. AUTOMATIC PROCESS CONTROL BY MODELS

The familiar troubles with the direct control of physicochemical processes at high temperatures lead us to the idea of mathematical models as exclusive sources of the melting process control. In addition, the mathematical models may also predict the desirable states and verify them almost instantly. At present, however, the parallel working of the model on the technologist's desk with the actual furnace is not feasible due to the complexity of melting processes and their numerous mutual relations. Fig. 9 is an attempt to describe the complex mathematical model for the process control with respect to the occurrence of glass defects and their elimination. As follows from Fig. 9, batch reactions and corrosion produce all kinds of glass defects, fuel combustion produces foam (reduction cond. f.e.), evaporation may produce both bubbles and heterogeneities, heterogeneities produce bubbles and refining may evoke foaming. The parallel courses of refining, particle dissolution and homogenization as well as their mutual linking (e.g. refining is linked to both particle dissolution and homogenization because of bubble nucleation, homogenization is linked to particle dissolution) are also indicated in Fig. 9. Batch feeding, fuel combustion, electrical heating and bubbles are main factors influencing glass flow. Glass flow, on the other hand, influences corrosion, refining, particle dissolution as well as homoge-

nization. Chemical composition of combustion gases may influence evaporation.

Much work has been done dealing with the construction of mathematical models up to now. The very informative paper of De Waal [58] is probably the latest exhausting review in the field. That is why only a brief survey of model evolution will be presented here and some selected aspects only mentioned.

The 3D model have been presented since the beginning of 1970's [59-61]. They include all-electric melting and boosting [52, 62-67], complex geometrical shapes [68], bubbling [53, 69, 70] and the residence time distribution [53]. Complex models have been developed e.g. by Ungan and Viskanta [65-67]. The historical development of 3D flow models is presented in the review by Nolet and Murname [71]. The main problems with the usability of 3D models have their origin not only in the need of extremely efficient computers with significant storage space, but also in unreliable data (heat conductivity) and limited possibilities of verification. Other sources of difficulties are the complex boundary conditions (this relates to sub-models), the complicated representation of 3D results (isolines, streak lines and velocity vectors in the perspective view, projections to 2D space, 2D cuts, coloured regions) and in neglecting some effects, as e.g. the glass surface vaulting [72]. Despite of the published analysis of glass flow in glassmelting furnaces [67], there is lack of papers dealing with simple flow models with fundamental flow patterns and their classification.

Hrma [73] and Schill [74] consider only one chemical reaction in the batch layer heated from below or from both sides to obtain a satisfactory description. As Hrma notes - despite of many useful conclusions - the degree of conversion in an actual melting tank

must, however, include several successive and partially overlapping reactions. The 2D model of Ungan and Viskanta [66] of two sides batch melting is probably the most sophisticated one. Although authors consider also batch conversion as a simple chemical reaction, useful information about the melting characteristics has been acquired. The main problem of the contemporary batch models is an insufficient description of the gas phase behaviour. The gas phase in the batch layer and the adjacent melt not only deeply changes the rheology of the batch [25] but also determines the initial heterogeneity distribution. Thorough experiments simulating time - temperature history inside of the batch blanket combined with sampling from industrial furnaces and subjected to detailed analysis (picture analysis e.g. for bubbles) may lead to a satisfactory semiempirical description.

Ungan [75] presents a sand dissolution of single classes of sand sizes coupled together. Nĕmec and Mühlbauer [76] presumed independence of instantaneous sand dissolution rate of particle size [77] using equation (7) for the calculation of the polydisperse sand concentration field in a glass furnace. As for dissolution of single refractory particles, Cooper's [78], Hrma's [6], Choudhary's [79] or Gamm's [80] equations have usually been applied. De Waal [58] and Orlov [81] give dimensionless relations including the effect of forced convection. There are, however, many troubles with a precise description if the gas phase participates in the particle dissolution. Bubbles are abundantly nucleated on sand grains owing to the gas supersaturation in regions enriched by  $\text{SiO}_2$  [5, 25] or in high temperature regions [17], distinctly accelerating sand dissolution and floating sand grains. Studies are therefore needed predicting nucleation intensity, especially special experimental measurements.

The first refining models have only considered one component single bubbles with a relatively simple behaviour [50, 82, 83]. Nĕmec [84] tried to express the bubble concentration field in the melting room using representatives of multicomponent bubbles. Ungan [67, 75], however, presented a model solving simultaneously the behaviour of ensemble one or two component bubbles and glass flow. As obvious from Simonis' work [85], the local distribution of diffusing species over the glass furnace has to be taken into account when calculating local redox equilibria of refining agents and diffusion of the refining gases between the bubble and the melt (Beerens [86]). Thus, the set of differential equations solved simultaneously to provide the picture of flow and refining includes the continuity, momentum and energy equations, the equations of the bubble ensemble behaviour [75], the refining species concentration equations [85] and the set of differential equations describing the behaviour of a multicomponent bubble

at given oxidation-reduction conditions. As already mentioned in Part 1.3., the physico-chemical aspects of refining must be taken into account when formulating the set of equations controlling the single bubble behaviour. In special productions (float glass), the low temperature refining models are needed. The values of mass transfer coefficients of appropriate gases are dependent strongly on the hydrodynamical conditions around the bubble [87]. The simplified models have also been applied using the experimental values of the bubble growth rates or results of laboratory bubble analysis. The first model fails, however, for a complicated time - temperature histories of bubbles, the second one is more appropriate for the identification of bubble sources (see later). The main problems of the refining models have their sources in the impact of bubbles on the glass flow, in the multicomponent gas diffusion between bubble and melt as well as in the changes of the refining agent concentration during glass melting (losses, accumulation). Besides laborious computations, a lot of experimental data are needed. Up to the present, little is exactly known about bubble nucleation and the size distribution of bubbles entering the melt.

The results mentioned in Part 1.4. form acceptable basis for the application to the glass furnaces. Goldberg [49] applied the results of Geffcken [88] and Becker [89] to calculate the reduction of the excess silica concentration along a furnace streamline, Rhiel [82, 90] starting from Cooper's results [57] derived a computer 3D model with a parallel effect of shear and rotation on heterogeneity attenuation and applied it to a glass furnace. Nevertheless, problems connected with the initial distribution and orientation of spacious heterogeneities remain.

Glass foam in a furnace may be produced by the decomposition reactions of carbonates [5, 91], reactions of refining agents with high silica glass melt [26] or by their thermal decomposition [17], by an interaction of the furnace atmosphere with the glass melt [41, 92], and mechanically (bubbling, stirring). The relative importance of individual decay mechanisms - the relative motion of bubbles, drainage, gas exchange and tear of liquid layers - is not quite clear, probably tear is the controlling process [91]. Considering that the stability of foam on the glass level is a result of the dynamical equilibrium between foam production and foam decay, the chemical factors also play an important role. The formulation of computer model is badly needed: under certain conditions, the whole glass melting process may be controlled by foam behaviour [20].

As for corrosion and evaporation models, they are outside the scope of this paper.

The contemporary mathematical models suffer above all from the insufficient knowledge of bubble

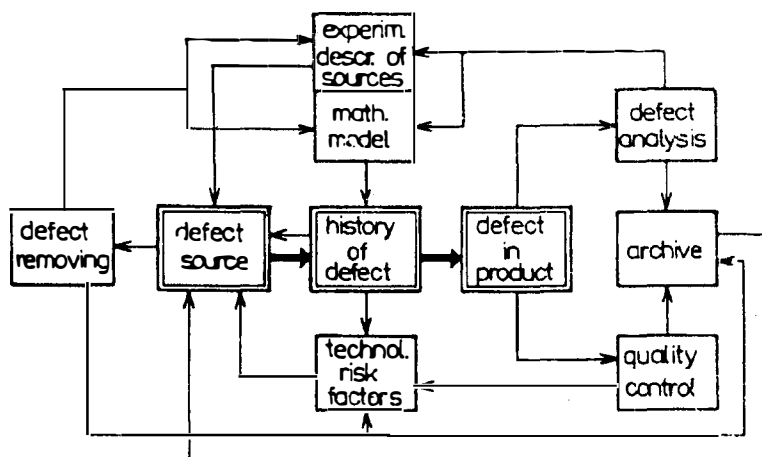


Fig. 10.: The scheme of the identification of glass melting defect.

→ actual development in glass furnace,

→| identification paths.

and foam behaviour during the melting process. Not with standing, there is no reason against their use in glass factories. The contemporary model may only be in this way continually corrected according to an actual furnace. It also represents an excellent expert being immediately available for the technologist.

### 3. IDENTIFICATION AND ELIMINATION OF GLASS DEFECT

Bubbles, stones and heterogeneities are the undesirable posterity of three main melting processes. Jebsen-Marwedel and Brückner [35] give a detailed description of defect sources, defect properties, history, defect analysis and methods how to eliminate them. Contemporary glass technologists dream, however, about automatic identification methods not demanding specialized knowledge or expensive analysis. It is the aim of this short chapter to sketch only a possible way how to do most of the specialized work in advance and how to use the actual technological data for bubble identification. The most straightforward way would be the use of mathematical modelling, namely so called backward modelling. However, the contemporary mathematical models of defect behaviour are mostly insufficiently precise for this subtle task or even not unambiguous.

The proposed automatic system for bubble source identification [93] uses therefore following sources of information:

- archives of resolved defect cases
- description of defect sources with respect to the technological risk factors
- results of the experimental (mathematical) modelling of the important sources at the expected time
- temperature histories.

The exploitation of the information sources, input data and information paths are obvious from Fig. 10.

The sequence of most probable sources is obtained from each information basis. The first two information bases make it possible to evaluate the potential bubble sources continuously using the collected technological risk parameters, the results of quality control and the archived identifications. The bubble sources have to be defined and the important ones are experimentally modelled (melting bubbles, air bubbles, CO<sub>2</sub> bubbles, bubbles from reduction) to construct the third information basis. A similar method for bubble identification was used for example by Krämer [94]. Every bubble source may thus be described by many properties facilitating its identification. Single bubble sources may be similarly described by the technological risk factors. Every successful solution will lead to an improvement of information bases. The main problem of the system is the necessary considerable amount of experimental work.

### CONCLUSION

The presented brief analysis of the glass melting process revealed that the application of controlled convection may lead to the improved heat transfer into the glass batch, enhanced sand dissolution as well as homogenization and consequently to the increased pull and decreased energy consumption as well as size of a glass melting room. The maximum melting temperatures may be lowered, but corrosion of refractory boundaries has to be thoroughly followed. Additional bubble elimination is necessary probably using physical ways of refining as reduced pressure or centrifugal force application. Thus, period of the glass

stired furnaces may be expected among new ways of glass melting. The principal problem consisting in the corresponding flow arrangement inside of the glass melting room remain, nevertheless, a challenge to the mathematical and physical modelling. In spite of verification and formulation problems of the contemporary mathematical models connected especially with the description of the gas phase behaviour, their cautious introducing into the glass industry represents the very promising way how to improve them and how to ensure process as well as quality control.

## References

- [1] Cooper A.R.: *Glass Technol.* 21, 87, (1980).
- [2] Némec L.: *Silikáty* 32, 193 (1988).
- [3] Bolta P., Radu D., Spurcaci C.: *Collected Papers of XIV. Int. Congr. on Glass, New Delhi, India, 16, (1986).*
- [4] Hrma P.: *Chemistry of Glass* aby A. Paul, Chapman and Hall. London and New York second ed., 157 (1988).
- [5] Hrma P.: *Proc. 1st Int. Conf. on Advances in the Fusion of Glass, Alfred, New York, 10.1. (1988).*
- [6] Hrma P.: *Silikáty* 24, 7 (1980).
- [7] Manfredo L.J., Mc Nally R.N.: *Com. Am. Ceram. Soc.* 8, C155 (1984).
- [8] Cooper A.R., Kingery W.D.: *J. Am. Ceram. Soc.* 47, 37 (1964).
- [9] Bushy T.S., Eccles J.: *Glass Technol.* 5, 115 (1964).
- [10] Schwerdtfeger K.: *J. Phys. Chem.* 70, 2131 (1966).
- [11] Hlaváč J., Nademlýnská H.: *Glass Technol.* 10, 54 (1969).
- [12] Truhlářová M., Vepřek O.: *Glastechn. Ber.* 40, 257 (1967).
- [13] Hrma P.: *Am. Ceram. Soc.* 68, 337 (1985).
- [14] Bodalbhai L., Hrma P.: *Glass Technol.* 27, 72 (1986).
- [15] Beneš J.: *The Kinetics of Silicate Glass Melting. Dr. Thesis, Inst. of Chem. Technol. Prague (1977).*
- [16] Hrma P., Bartoň J., Tolt T.L.: *J. Non-Cryst. Solids* 84, 370 (1986).
- [17] Némec L.: *J. Am. Ceram. Soc.* 60, 436 (1977).
- [18] Mühlbauer M., Némec L.: *Am. Ceram. Soc. Bull.* 64, 1471 (1985).
- [19] Némec L.: *Sklář a keram.* 29, 104 (1979).
- [20] Hrma P.: *Glastechn. Ber.* 63K, 360 (1990).
- [21] Richards R.S.: *Ceramic Bull.* 67, 1806 (1988).
- [22] Cable M., Clarke A.R., Haroon M.A.: *Glass Technol.* 10, 15 (1969).
- [23] Cable M., Clarke A.R., Haroon M.A.: *Glass Technol.* 9, 101 (1968).
- [24] Mulfinger H.O.: *Glastechn. Ber.* 49, 232 (1976).
- [25] Dor-Sang Kim, Hrma P.: *Ceram. Bull.* 69, 1039 (1990).
- [26] Don-Sang Kim, Hrma P.: *J. Am. Ceram. Soc.* 74 551 (1991).
- [27] Némec L.: *Glass Technol.* 15, 153 (1974).
- [28] Némec L.: *Sklář a keram.* 23, 263 (1973).
- [29] Némec L.: *Glass Technol.* 21, 134 (1980).
- [30] Némec L., Mühlbauer M.: *Glastechn. Ber.* 54, 99 (1981).
- [31] Krämer F.: *Glastechn. Ber.* 53, 177 (1980).
- [32] El Harfoui M., Hilger J.P.: *Glastechn. Ber.* 64, 253 (1991).
- [33] Mulfinger H.O., Meyer H.: *Glastechn. Ber.* 36, 481 (1963).
- [34] Richardson F.D.: *Physical Chemistry of Melts in Metallurgy*, Volume 2, Academic Press, London - New York, 292 (1974).
- [35] Jebesen-Marwedel H., Brückner R.: *Glastechnische Fabrikationsfehler*, Springer Verlag Berlin-Heidelberg-New York, 242 (1980).
- [36] Ullrich J., Némec L.: *Identification of Bubble Sources in Flat Glass, Internal Report of Glass Service Ltd., for Glav Union Teplice (1991).*
- [37] Golob H.R., Swarts E.L.: *J. Am. Ceram. Soc.* 67, 564 (1984).
- [38] Plumet E., Toussaint S., Boffe M.: *J. Am. Ceram. Soc.* 49, 551 (1966).
- [39] Matěj J., Némec L., Freivolt M.: *Proceedings of VII Conf. on Electric Melting of Glass, Prague, 52 (1986).*
- [40] Cable M., Rasul C.G.: *J. Am. Ceram. Soc.* 50, 528 (1968).
- [41] Hanke K.P.: *Glastechn. Ber.* 50, 144 (1977).
- [42] Holmquist S.: *J. Am. Ceram. Soc.* 49, 467 (1966).
- [43] Némec L.: *Glass Technol.* 21, 139 (1980).
- [44] Schreiber H.D., Kozak S.J., Fritchman A.L., Goldman D.S., Schaeffer H.A.: *Phys. Chem. Glasses* 27, 152 (1986)
- [45] Némec L., Schill P., Chmelař J.: *to be published in Glastechn. Ber. (1992).*
- [46] Turzynski W.: *Szklo i ceramika* 7, 196 (1961).
- [47] Pankova N.A., Koloskova O.I., Prochorov B.N.: *Collected Papers of XIV Int. Congr. on Glass, New Delhi India, 42 (1986).*
- [48] Kishigami H.: *Yogyo-Kyokai-Shi* 79, 105 (1971).
- [49] Goldberg A.J.: *Glastechn. Ber.* 46, 67 (1973).
- [50] Suzuki J., Kato T., Mishima M.: *J. Non-Cryst. Solids* 38, 39, 861 (1980).
- [51] Némec L., Schill P., Chmelař J.: *The Influence of Temperature Field of Glass Flow in a Horizontal Melting Room. 1st Int. Conf. Fundamentals of the Glass Manufacturing Process, Sheffield (1991).*
- [52] Choudhary M.K.: *J. Non-Cryst. Solid* 101, 41 (1988).
- [53] Simonis F., De Waal H., Beerkens R.C.G.: *Collected Papers of XIV. Int. COng. on Glass, New Delhi, p. 118 (1986).*
- [54] Némec L.: *Sklář a keram.* 29, 144 (1979).
- [55] Cooper A.R.: *Collected Papers of XIV. Int. Congr. on Glass, New Delhi, p. 1 (1986).*
- [56] Cooper A.R.: *Proc. 2st Int. Conf. on Advances in the Fusion of Glass, Alfred, New York p. 23.1., (1988).*
- [57] Cooper A.R.: *Chem. Eng. Sci.* 21, 1095 (1966).
- [58] De Waal H.: *Glastechn. Ber.* 63K, 1 (1990).
- [59] Chen T., Goodson R.E.: *Glass Technol.* 13, 161 (1972).
- [60] Moulton A.: *Glass Technol.* 23, 106 (1982).
- [61] Carling J.C.: *Glass Technol.* 23, 201 (1982).
- [62] Philip G.: *Silikattechnik* 37, 12, (1986).
- [63] Hilbig G.: *Glastechn. Ber.* 63, 185 (1990).
- [64] Hilbig G.: *Proc. of 11 Ibausil Weimar, p. 631 (1991).*

- [65] Urgan A., Viskanta R.: *Glass Technol.* **28**, p. 252 (1987).
- [66] Urgan A., Viskanta R.: *Glastechn. Ber.* **59**, 279 (1986).
- [67] Urgan A., Viskanta R.: *Glastechn. Ber.* **60**, 71, 115 (1987).
- [68] Schill P.: XVI Int. Congr. on Glass, Vol. 6, p. 31, Madrid (1992).
- [69] Urgan A., Viskanta R.: *J. Am. Ceram. Soc.* **69**, 382 (1986).
- [70] Carvalho M.G., Nogueira M.: *Mathematical Modelling of Heat of the Glass Manufacturing Process*, 1st Int. Conf. Fundamentals of the Glass Manufacturing Process, Sheffield (1991).
- [71] Nolet D.A., Murname R.A.: *Proc. 1st Int. Conf. on Advances in the Fusion of Glass*, Alfred, New York, p. 13.1. (1988).
- [72] Trier W.: *Proc. of 11 Ibausil, Weimar*, p. 569 (1991).
- [73] Hrma P.: *Glastechn. Ber.* **55**, 138 (1982).
- [74] Schill P.: *Silikáty* **30**, 107, (1986).
- [75] Urgan A.: *Glastechn. Ber.* **63K**, 19 (1990).
- [76] Němec L., Mühlbauer M.: *Glastechn. Ber.* **56K**, 82 (1983).
- [77] Freivolt Š., Němec L.: *Silikáty* **29**, 215 (1985).
- [78] Cooper A.R.: *Chem. Eng. Sci.* **21**, 917 (1966).
- [79] Choudhary M.K.: *Glass Technol.* **29**, 100 (1988).
- [80] Gamm H.D.: *Mass Transfer Problems in Glass Furnace Simulation*. ScD. Thesis, M.I.T., Cambridge, Massachusetts (1975).
- [81] Orlov D.L.: *Proceedings of XV Int. Congr. on Glass*, Survey Papers, p. 442 (1989).
- [82] Rhiel F.R.: *Dr. Thesis, Theinisch Westfällischen Hochschule Aachen* (1976).
- [83] Štefan J., Škřivan M., Fojtíková M.: *Sklář a keram.* **29**, 166 (1979).
- [84] Němec L.: *Bubble Concentration Field in the Glass Melting Furnace*. Report of the State Project of Fundamental Research No. IV-4-3/02. Institute of Glass Chemistry Prague (1983).
- [85] Simonis F.: *Glastechn. Ber.* **63K**, 29 (1990).
- [86] Beerkens R.C.G.: *Glastechn. Ber.* **63K**, 222 (1990).
- [87] Chmelář J.: *Collected Papers of the 1st Int. Seminar on Math. Simulation in the Glassmelting*. Valašské Meziříčí, p. 32 (1991).
- [88] Geffcken W.: *Glastechn. Ber.* **30**, 143 (1957).
- [89] Becker H.: *Glastechn. Ber.* **35**, 387 (1962).
- [90] Rhiel F.F.: *Glastechn. Ber.* **49**, 217 (1976).
- [91] Kappel J., Conradt R., Scholze H.: *Glastechn. Ber.* **60**, 189 (1987).
- [92] Hanke K.P., Scholze H.: *Glastechn. Ber.* **43** 475 (1970).
- [93] Chmelář J., Němec L., Frank A.: *Control of Glass Quality Using 3D Modelling*. 3rd Int. Conf. on Advances in Glass Melting, New Orleans, June (1992).
- [94] Krämer F.: *Collected Papers of the XIV Int. Congr. on Glass*, New Delhi, India, p. 288, (1986).

Submitted in English by the author